and $\phi = \phi_1 - \phi_2$ and again $n = -i\partial/\partial\phi$ and $\phi = i\partial/\partial n$. Thus, locally there is a superposition of different n states: ϕ is fixed so n is uncertain. It is clear that there must be a dividing line between these two behaviors, perfect phase coherence and negligible coherence, namely the Josephson effect.

Clearly, again, the total phase of the assembly is not physical. However, the relative phases can be given a meaning when one observes, as one does in e.g. metallic superconductors, that electrons can pass back and forth through the barrier, leading to the possibility of coherence between states in which the total number of electrons is not fixed *locally*. Under such conditions there is, for instance, a coherence between the state with $N/2$ electrons in one half of the block and $N/2$ in the other, and that with $(N/2) + 2$ on one side side and $(N/2) - 2$ on the other.

In the nuclear case, one can view the systems $|BCS(A+2)\rangle$ and $|BCS(A)\rangle$ as parts of a fermion superfluid (superconductor) which, in presence of a proton $(p + (A+2))$ are in weak contact to each other, the $d + |BCS(A+1)\rangle$ system (without scattering, running waves, but as a closed, virtual, channel) acting as the dioxide layer of a Josephson junction (Fig. 3.7.1).

Under favorable conditions, in particular of Q–value for the different channels involved and, similarly to the so called backwards rise effect, one may, arguably, observe signals of the coherence between systems $(A+2)$ and A in the elastic scattering process ${}^{A+2}X + p \rightarrow ({}^{A}X + t) \rightarrow {}^{A+2}X$, ${}^{i}X$ denoting a member of a pairing rotational band (cf. Fig. 3.7.1, see also Fig 2.1.3).

Whether an effect which may parallel that shown in (c) (backwards rise) can be seen or not depends on a number of factors, but very likely it is expected to be a weak effect. This was also true in the case of the Josephson effect in its varied versions (AC, DC, etc.). In fact, its observation required to take into account the effect of the earth magnetic field, let alone quantal and thermal fluctuations.

A direct observation of weak coupling coherent phenomena between states $|BCS(A+2)\rangle$ and $|BCS(A)\rangle$ in $A + a \rightarrow A + a$ process could arguably, be achieved in e.g. the virtual transfer of two protons in the case in which the system A is superfluid in Z, and of the observation of associated γ–rays of frequency $\nu = Q_{2p}/h$, where Q_{2p} is the Q-value of the two proton transfer process. It is of notice that a similar effect will be observed in the case of of two-neutron transfer between superfluid systems in N, in keeping with the neutron effective charge.

3.8 Hindsight

The formulation of superconductivity (BCS theory) described by Gor'kov[57] allows, among other things for a simple visualization of spatial dependences. In this formulation $F(\mathbf{x}, \mathbf{x}')$ is the amplitude for two Fermions (electrons) at $\mathbf{x}, \mathbf{x}'$, to belong to the Cooper pair (within the framework of nuclear physics cf. e.g. Fig. 2.6.3 $\Psi_0(\mathbf{r}_1, \mathbf{r}_2)$; see also App. 3.B). The phase of F is closely related to the angular orientation of the spin variable in Anderson's quasispin formulation of BCS theory[58].

[57] Gor'kov (1958); Gor'kov, L.P. (1959).

[58] Anderson (1958); within the framework of nuclear physics cf. e.g. Bohr and Ulfbeck (1988), Potel, G. et al. (2013b) and references therein.

The gap function $\Delta(x)$ is given by $V(\mathbf{x})F(\mathbf{x},\mathbf{x})$ where $V(\mathbf{x})$ is the local two–body interaction at the point $\mathbf{x}$. In the insulating barrier between the two superconductors of a Josephson junction, $V(\mathbf{x})$ is zero and thus $\Delta(x)$ is also zero.

The crucial point is that vanishing[59] $\Delta(x)$ does not imply vanishing F, provided, of course, that one has within the insulating barrier, a non–zero particle (electron) density, resulting from the overlap of densities from right (R) and left (L) superconductors. Now, these barriers are such that they allow for one–electron–tunneling with a probability of the order of 10^{-10} and, consequently, the above requirement is fulfilled. Nonetheless, conventional (normal) simultaneous pair transfer, with a probability of $(10^{-10})^2$ will not be observed[60]. But because one electron at a time can tunnel profiting of the small, but finite electron density within the layer, $F(\mathbf{x},\mathbf{x}')$ can have large amplitude for Cooper pairs with partners electrons one on each side of the barrier (i.e. $\mathbf{x} \in$ L and $\mathbf{x}' \in$ R), separated by distances $|\mathbf{x}-\mathbf{x}'|$ up to the coherence length. Hence, for barriers thick to only allow for essentially ~~the tun-neling~~ of one electron at a time, but thin ~~compared with the~~ coherence length, two electrons on opposite sides of ~~the barrier~~ can still be correlated and the pair current ~~can~~ be consistent. An evaluation of its value shows that, at zero temperature, the pair current is equal to the single particle current at an equivalent voltage[61] ~~$\pi\Delta/2e$~~.

$\pi/4$ times

$2\Delta/e$

e

The translation of the above parlance to the language of nuclear physics has to come to terms with the basic fact that nuclei are self–bound, finite many–body systems in which the surface, as well as space quantization, play a very important role both as a static element of confinement, as well as a dynamic source for renormalization effects[62,63]. Under the influence of the average potential which can be viewed as very strong external field ($|V_0| \approx 50$ MeV), Cooper pairs ($|E_{corr}| \approx 1.5$ MeV; see e.g. Fig. 2.5.1) will become constrained within its boundaries with some amount of spill out. In the case of the single open shell superfluid nucleus ^{120}Sn, the boundary can be characterized by the radius $R_0 \approx 6$ fm ($\ll \xi \approx 14$ fm), the spill out being connected with the diffusivity $a \approx 0.65$ fm.

Let us now consider a two nucleon transfer reaction in the collision Sn+Sn

---

[59] This point was likely misunderstood by Bardeen who writes"... In my view, virtual pair excitations do not extend across the layer...", see McDonald (2001), see also Bardeen (1961) and Bardeen (1962).

[60] Pippard (2012) see also McDonald (2001).

[61] In the case of Pb at low temperatures ($\approx$ 7.19 K (0.62 meV)) this voltage is ≈ 1 meV/e = 1 mV leading to $\approx$2mA current for a barrier resistance of $R \sim 1\Omega$ (Ambegaokar and Baratoff (1963); McDonald (2001); Tinkham (1996)).

[62] Within this context it is of notice that the liquid drop model is a very successful nuclear model, able to accurately describe not only large amplitude motion (fission, exotic decay, low–lying collective density and surface vibrations, cf. e.g. Bohr and Wheeler (1939), Barranco, F. et al. (1990), Bertsch (1988), see also Brink, D. and Broglia (2005) and references therein), but also the masses of nuclides (see e.g. Møller, P. *et al.* (1995)), provided the superfluid inertia and shell corrections respectively, are properly considered. Thus, it is an open question whether in the quest of developing more predictive theoretical tools of the global nuclear properties one should develop ever more "accurate" zero range (Skyrme–like) forces, or deal also with the long wavelength, renormalization effects and induced interaction.

[63] Broglia, R. A. (2002).

Ricardo.
Send scanning final
Fig.
red
put horizontal
so there is
enough space
and caption
eventually
next
page

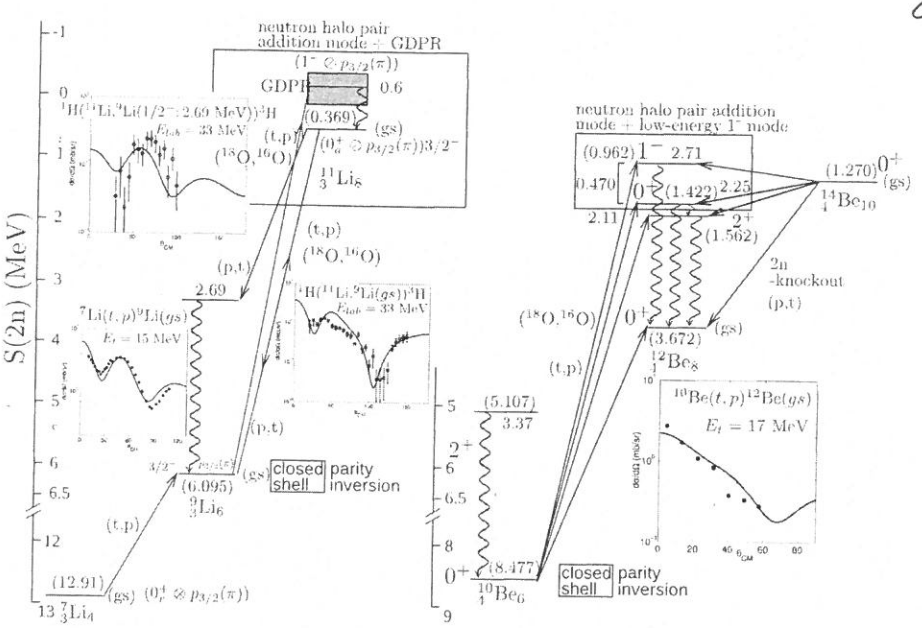

Figure 3.8.1: Monopole pairing vibrational modes associated with $N = 6$ parity inverted closed shell isotones, together with low-energy E1-strength modes. The levels are displayed as a function of the two-neutron separation energies $S(2n)$. These quantities are shown in parenthesis on each level, the excitation energies with respect to the ground state are quoted in MeV. Absolute differential cross sections from selected (t, p) and (p, t) reactions calculated as described in the text (cf. Potel et al. (2010, 2014)), in comparison with the experimental data (Young and Stokes (1971); Fortune et al. (1994)).

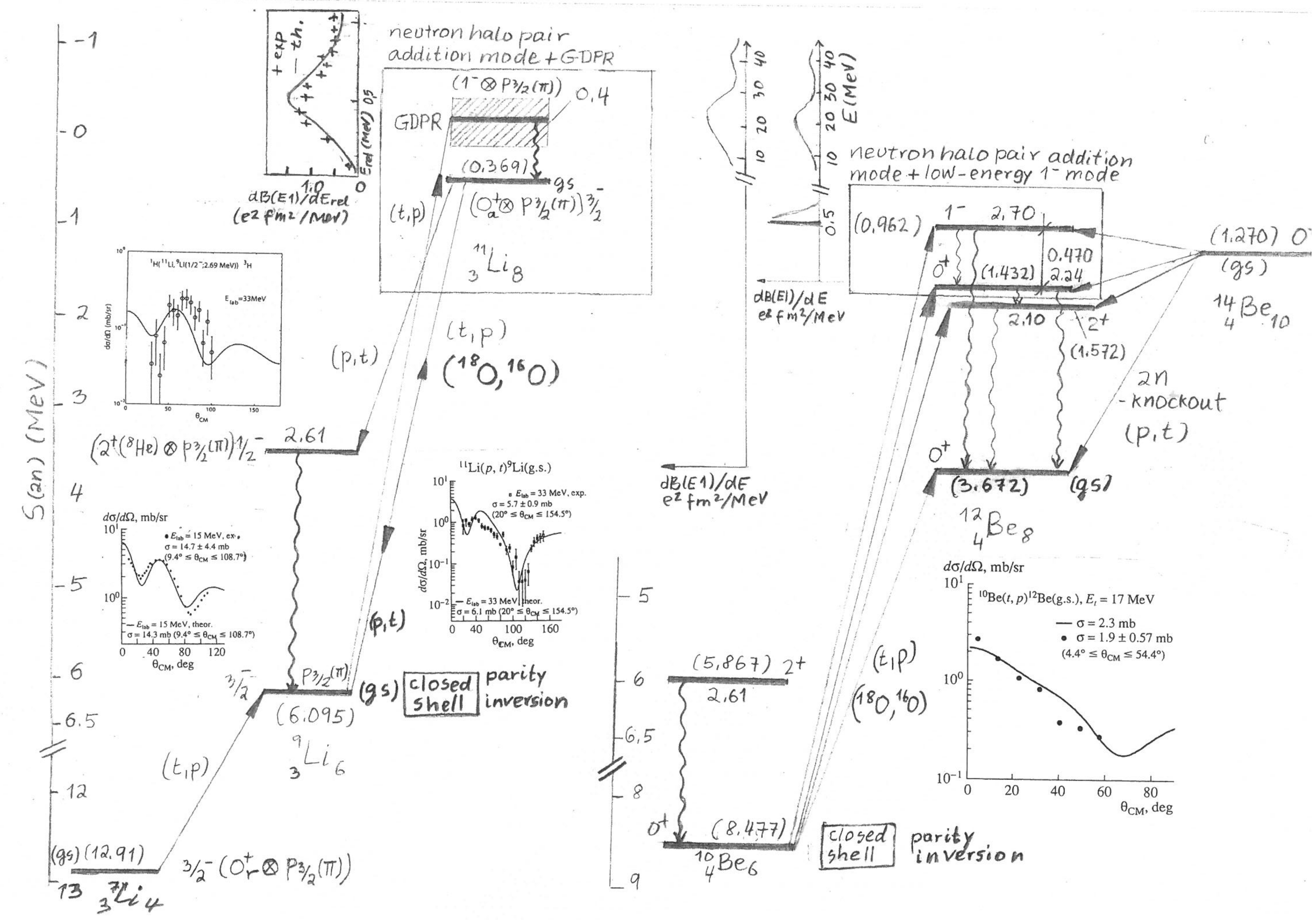

S(2n) (MeV)
neutron halo pair addition mode + GDPR
GDPR
$(1^- \otimes p_{3/2}(\pi))$
0.4
(0.369)
gs
$(0^+_a \otimes p_{3/2}(\pi))\,3/2^-$
(t,p)
$^{11}_{3}Li_8$
+ exp
— th.
dB(E1)/dErel (e² fm² /MeV)
Erel (MeV)
$^1H(^{11}Li,\,^9Li(1/2^-;2.69\ MeV))\,^3H$
E_{lab}=33MeV
dσ/dΩ (mb/sr)
θ_{CM}
(p,t)
(t,p)
(^{18}O,^{16}O)
$(2^+(^8He) \otimes p_{3/2}(\pi))\,1/2^-$
2.61
$p_{3/2}(\pi)$
$3/2^-$
(gs)
closed shell
parity inversion
(6.095)
$^9_3Li_6$
(p,t)
$^{11}Li(p,t)^9Li(g.s.)$
E_{lab} = 33 MeV, exp.
σ = 5.7 ± 0.9 mb
(20° ≤ θ_{CM} ≤ 154.5°)
— E_{lab} = 33 MeV, theor.
σ = 6.1 mb (20° ≤ θ_{CM} ≤ 154.5°)
dσ/dΩ, mb/sr
θ_{CM}, deg
dσ/dΩ, mb/sr
● E_{lab} = 15 MeV, exp.
σ = 14.7 ± 4.4 mb
(9.4° ≤ θ_{CM} ≤ 108.7°)
— E_{lab} = 15 MeV, theor.
σ = 14.3 mb (9.4° ≤ θ_{CM} ≤ 108.7°)
θ_{CM}, deg
(t,p)
(gs) (12.91)
$3/2^-(0^+_r \otimes p_{3/2}(\pi))$
$^7_3Li_4$
dB(E1)/dE e² fm²/MeV
E(MeV)
neutron halo pair addition mode + low-energy 1⁻ mode
(0.962)
1⁻
2.70
0⁺
(1.432)
0.470
2.24
2.10
2⁺
(1.572)
(1.270) 0⁺
(gs)
$^{14}_{4}Be_{10}$
2n -knockout
(p,t)
0⁺
(3.672)
(gs)
$^{12}_{4}Be_8$
dσ/dΩ, mb/sr
$^{10}Be(t,p)^{12}Be(g.s.)$, E_t = 17 MeV
— σ = 2.3 mb
● σ = 1.9 ± 0.57 mb
(4.4° ≤ θ_{CM} ≤ 54.4°)
θ_{CM}, deg
(t,p)
(^{18}O,^{16}O)
(5.867) 2⁺
2.61
0⁺
(8.477)
$^{10}_{4}Be_6$
closed shell
parity inversion

In many-body systems, medium polarization effects play an important role in renormalising single-particle motion and four-point vertices, namely the Coulomb interaction in condensed matter, and the bare NN-potential in nuclei. In what follows special attention is paid to medium

polarization effect in connection with the pairing interaction

3.A.1 Nuclei

Polarization contributions to the bare nucleon–nucleon pairing interaction through elementary modes of excitation

Elementary modes of excitation constitute a basis of states in which correlations, as found in observables, play an important role. As a consequence, it allows for an economic solution of the nuclear many–body problem of structure and reaction. A first step in this quest is to eliminate the non–orthogonality associated with single–particle motion in different nuclei (target and projectile (*reaction*)). Also between single–particle degrees of freedom and collective modes (vibrations and rotations (*structure*)) typical of an overcomplete , Pauli principle violating, basis. This can be done by diagonalizing, making use of the rules of nuclear field theory (NFT), the particle–vibration coupling (PVC), and the v_{np} (v : four point vertex, bare NN–) interaction. In this way one obtains quantities (energies, transition probabilities, absolute value of reaction cross sections) which can be directly compared with the experimental findings. Such a protocol can be carried out, in most cases, within the framework of perturbation theory. For example, second order perturbation theory, in both reaction and structure, as exemplified in Fig. 1.9.3 displaying a NFT (r+s) graphical representation of contributions to the ^{11}Li$(p,t)^9$Li(gs) and ^{11}Li$(p,t)^9$Li($1/2^-$;2.69 MeV) processes (see also Fig. 6.1.3). As a result, single-particle states move in a gas of vibrational quanta and become clothed by coupling to them. Similar couplings renormalize the bare NN–interaction in the different channels. In particular in the $^1S_0$ (pairing) channel.

Also as a result of their interweaving, the variety of elementary modes of excitation may break in a number of states, eventually acquiring a lifetime and, within a coarse grain approximation, a damping width (imaginary component of the self energy). Moving into the continuum, as for example in the case of direct reactions, one such component is the imaginary part of the optical potential operating in the particular channel selected. It can be calculated microscopically using similar techniques and elements as e.g. those used in the calculation of the damping width of giant resonances. With the help of dispersion relations, the real part of the optical potential can be obtained from the knowledge of the energy dependence of the absorptive potential. In this way, the consistency circle structure–reaction based on elementary modes and codified by NFT could be closed. The rich variety of emergent properties found along the way eventually acquiring a conspicuous level of physical validation. In the case of halo exotic nuclei, in particular in the case of ^{11}Li (bootstrap, Van der Waals Cooper binding, halo pair addition mode (symbiosis of pairing vibration and pygmy) being few of the associated emergent properties) one is rather close to his goal. At that time it would be possible, arguably if there is one, to posit that the *ultima ratio* of structure and reactions, in any case that associated with pairing and Cooper pair transfer in nuclei, have been unveiled[65]

[65]In the above paragraph we allowed ourselves to paraphrase Jacques Monod writing in connection with biology and life: L'*ultima ratio* de toutes les structures et performances téléonomiques

this

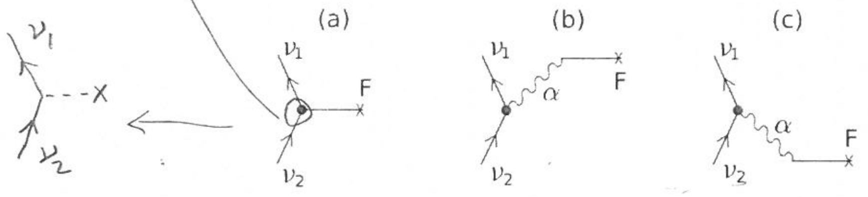

Figure 3.A.1: (a) F–moment of single–particle and (b,c) renormalization effects induced by the collective vibration α.

Effective moments

At the basis of the coupling between elementary modes of excitation, for example of single–particle motion and of collective vibrations, one finds the fact that, in describing the nuclear structure it is necessary to make reference to both of them simultaneously and in an unified way.

Within the harmonic approximation the above statement is economically embodied in e.g. the relation existing between the collective ($\hat{\alpha}$) and the single–particle ($\hat{F}$) representation of the operator creating a particle–hole excitation. That is[66],

$$
\begin{aligned}
\hat{F} &= \left\{ \langle k|F|\tilde{i}\rangle \Gamma^{\dagger}_{ki} + \langle \tilde{i}|F|k\rangle \Gamma_{ki} \right\} \\
&= \sum_{k,i,\alpha'} X^{\alpha'}_{ki}\Gamma^{\dagger}_{\alpha'} - Y^{\alpha'}_{ki}\Gamma_{\alpha'} \\
&= \sum_{\alpha'} \Lambda_{\alpha'} \sum_{ki} \frac{\left|\langle \tilde{i}|F|k\rangle\right|^2 2(\epsilon_i - \epsilon_k)}{(\epsilon_k - \epsilon_i)^2 - (\hbar\omega_{\alpha'})^2} \left(\Gamma^{\dagger}_{\alpha'} + \Gamma_{\alpha'}\right) \\
&= \sum_{\alpha'} \frac{\Lambda_{\alpha'}}{\kappa} \left(\Gamma^{\dagger}_{\alpha'} + \Gamma_{\alpha'}\right) = \sum_{\alpha'} \sqrt{\frac{\hbar\omega_{\alpha'}}{2C'_{\alpha}}} \left(\Gamma^{\dagger}_{\alpha'} + \Gamma_{\alpha'}\right) = \hat{\alpha}.
\end{aligned} \tag{3.A.1}
$$

This is a consequence of the self consistent relation

$$\delta U(r) = \int d\mathbf{r}' \delta\rho(r) v(|\mathbf{r}-\mathbf{r}'|), \tag{3.A.2}$$

existing between density (collective) and potential (single–particle) distortion, typical of normal modes of many–body systems.

Relation (3.A.1) implies that at the basis of these normal modes one finds the (attractive $\kappa < 0$) separable interaction

$$H = \frac{\kappa}{2}\hat{F}\hat{F}, \tag{3.A.3}$$

des êtres vivants est donc enfermée dans les séquences des radicaux des fibres polypeptidiques "embryons" de ces démons de Maxwell biologiques que sont les protéines globulaires. En un sens, très réel, c'est à ce niveau d'organisation chimique qui gît, s'il y en a un, le secret de la vie. Et saurait–on non seullement décrire les séquences, mais énoncer la loi d'assemblage à laquelle obéissent, on pourrait dire que le secret est percé, l'ultima ratio découverte (Monod (1970)).

[66] cf. Bohr, A. and Mottelson (1975), cf. also Brink, D. and Broglia (2005) App. C.

$\Lambda_\alpha = \kappa \sqrt{\frac{\hbar\omega_\alpha}{2C_\alpha}}$ $\kappa < 0$ $(\Lambda_\alpha < 0)$

$\delta U = \int dr' \delta\rho\, v < 0$ $(v < 0)$

but where now (Fig. 3.A.1 (a))

$$\hat{F} = \sum_{\nu_1,\nu_2} \langle \nu_1|F|\nu_2\rangle a^\dagger_{\nu_1} a_{\nu_2}, \tag{3.A.4}$$

is a general single–particle operator, while $\hat{F}$ in Eq. (3.A.1) is its harmonic representation acting in the particle (k)–hole (i) space, $\Gamma^\dagger_{ki}$ and Γ_{ki} being (quasi) bosons, i.e. respecting the commutation relation

$$\left[\Gamma_{ki}, \Gamma^\dagger_{k'i'}\right] = \delta(k,k')\delta(i,i'). \tag{3.A.5}$$

In other words, the representation (3.A.1), which is at the basis of the RPA (as well as QRPA), does not allow for scattering vertices, processes which become operative by rewriting (3.A.3) in terms of the particle–vibration coupling Hamiltonian

$$H_c = \kappa\hat{\alpha}\hat{F} \tag{3.A.6}$$

italics

It is of notice that κ is negative for an attractive field. Let us now calculate the effective single–particle moments (cf. Fig. 3.A.1 (b)),

$$\begin{aligned}
\langle \nu_2|\hat{F}|\nu_1\rangle_{(b)} &= \frac{\langle \nu_2|\hat{F}|\nu_2, n_\alpha = 1\rangle\langle \nu_2, n_\alpha = 1|H_c|\nu_1\rangle}{(\epsilon_{\nu_1} - \epsilon_{\nu_2}) - \hbar\omega_\alpha}, \\
&= \frac{\langle 0|\hat{\alpha}|n_\alpha = 1\rangle\kappa\alpha\langle \nu_2|F|\nu_1\rangle}{(\epsilon_{\nu_1} - \epsilon_{\nu_2}) - \hbar\omega_\alpha}, \\
&= \kappa\alpha^2 \frac{\langle \nu_2|F|\nu_1\rangle}{(\epsilon_{\nu_1} - \epsilon_{\nu_2}) - \hbar\omega_\alpha},
\end{aligned} \tag{3.A.7}$$

and (Fig. 3.A.1 (c))[67]

$$\begin{aligned}
\langle \nu_2|\hat{F}|\nu_1\rangle_{(c)} &= \frac{\langle \nu_2|H_c|\nu_1, n_\alpha = 1\rangle\langle \nu_1, n_\alpha = 1|F|\nu_1\rangle}{\epsilon_{\nu_2} - (\epsilon_{\nu_1} + \hbar\omega_\alpha)}, \\
&= \kappa\alpha^2\left(-\frac{\langle \nu_2|F|\nu_1\rangle}{(\epsilon_{\nu_1} - \epsilon_{\nu_2}) + \hbar\omega_\alpha}\right),
\end{aligned} \tag{3.A.8}$$

leading to

$$\begin{aligned}
\langle \nu_2|\hat{F}|\nu_1\rangle_{(b)} + \langle \nu_2|\hat{F}|\nu_1\rangle_{(c)} &= \kappa\alpha^2 \frac{2\hbar\omega_\alpha\langle \nu_2|F|\nu_1\rangle}{(\epsilon_{\nu_1} - \epsilon_{\nu_2})^2 - (\hbar\omega_\alpha)^2}, \\
&= \frac{\kappa}{C_\alpha}\frac{(\hbar\omega_\alpha)^2\langle \nu_2|F|\nu_1\rangle}{(\epsilon_{\nu_1} - \epsilon_{\nu_2})^2 - (\hbar\omega_\alpha)^2}.
\end{aligned} \tag{3.A.9}$$

[67] In calculating the energy denominators one takes the difference between the energy of the initial and of the intermediate states. However, when an external field like $\hat{F}$ acts on the system, before the PVC or four-point vertices operate, being equivalent to an observation, the energy denominator is to be calculated as the energy difference between the final and the intermediate states.

This is in keeping with the fact that the ZPF of the α–vibrational mode is,

$$\alpha = \sqrt{\frac{\hbar\omega_\alpha}{2C_\alpha}}, \tag{3.A.10}$$

the particle–vibration coupling strength being

$$\Lambda_\alpha = \kappa\alpha. \tag{3.A.11}$$

Together with $\langle\nu_2|\hat{F}|\nu_1\rangle_{(a)} = \langle\nu_2|F|\nu_1\rangle$ (see Fig. 3.A.1 (a)) one obtains

$$\langle\nu_2|\hat{F}|\nu_1\rangle = (1 + \chi(\omega))\,\langle\nu_2|F|\nu_1\rangle, \tag{3.A.12}$$

where

$$\chi_\alpha(\omega) = \frac{\kappa}{C_\alpha}\frac{\omega_\alpha^2}{\omega^2 - \omega_\alpha^2} \tag{3.A.13}$$

is the polarizability coefficient while

$$\omega = |\epsilon_{\nu_1} - \epsilon_{\nu_2}|/\hbar. \tag{3.A.14}$$

In the static limit, e.g. in the case in which α is a giant resonance and $\omega_\alpha \gg \omega$ one obtains

$$\chi_\alpha(0) = -\frac{\kappa}{C_\alpha}. \tag{3.A.15}$$

The sign of $\chi_\alpha(0)$ is opposite to that of κ, since the static polarization effect produced by an attractive coupling ($\kappa < 0$) is in phase with the single–particle moment, while a repulsive coupling ($\kappa > 0$) implies opposite phases for the polarization effect and the one–particle moment[68].

Let us now calculate the two–body pairing induced interaction (Fig. 3.A.2) arising from the exchange of collective vibrations[69] (summing over the two time orderings and symmetrizing between initial and final states)[70]

$$\begin{aligned}
v^{ind}_{\nu\nu'}(a) + v^{ind}_{\nu\nu'}(b) &= \kappa^2\alpha^2\left|\langle\nu'|F|\nu\rangle\right|^2\left(\frac{1}{\epsilon_\nu - \epsilon_{\nu'} - \hbar\omega_\alpha} + \frac{1}{\epsilon_{\nu'} - \epsilon_\nu - \hbar\omega_\alpha}\right),\\
&= \kappa^2\alpha^2\left|\langle\nu'|F|\nu\rangle\right|^2\left(\frac{1}{(\epsilon_\nu - \epsilon_{\nu'}) - \hbar\omega_\alpha} - \frac{1}{(\epsilon_\nu - \epsilon_{\nu'}) + \hbar\omega_\alpha}\right),\\
&= \Lambda_\alpha^2\left|\langle\nu'|F|\nu\rangle\right|^2\left(\frac{2\hbar\omega_\alpha}{(\epsilon_\nu - \epsilon_{\nu'})^2 - (\hbar\omega_\alpha)^2}\right),\\
&= v^{ind}_{\nu\nu'}(c) + v^{ind}_{\nu\nu'}(d).
\end{aligned} \tag{3.A.16}$$

Thus

[68] Bohr, A. and Mottelson (1975); Mottelson (1962).

[69] In the present discussion we do not consider spin modes. For details see e.g. Idini et al. (2015). See also Bortignon et al. (1983).

[70] Cf. Brink, D. and Broglia (2005) p. 217.

Think in the first case about the effect the GQR ($\tau=0$) plays in $(e(E2))_{eff}$ and, in the second ~~that~~ played by the GDR ($\tau=1$) in $(e(E1))_{eff}$

$$K\,|\langle \nu'|F|\nu\rangle|^2 + \frac{K^2}{C_\alpha}|\langle \nu'|F|\nu\rangle|^2\,\frac{(\hbar\omega_\alpha)^2}{\omega^2-\omega_\alpha^2}$$

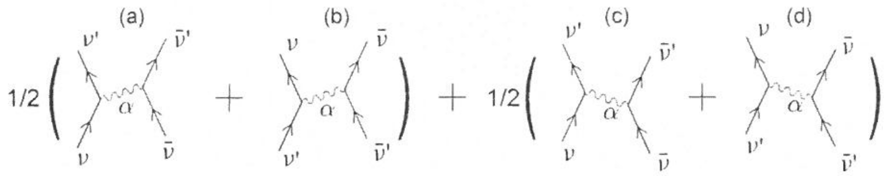

Figure 3.A.2: Diagrams associated with nuclear pairing induced interaction.

$$\begin{aligned} v^{ind}_{\nu\nu'} &= \frac{1}{2}\left(v^{ind}_{\nu\nu'}(a) + v^{ind}_{\nu\nu'}(b)\right) + \frac{1}{2}\left(v^{ind}_{\nu\nu'}(c) + v^{ind}_{\nu\nu'}(d)\right) \\ &= \Lambda_\alpha^2 \left|\langle \nu'|F|\nu\rangle\right|^2 \left(\frac{2\hbar\omega_\alpha}{\omega^2 - (\hbar\omega_\alpha)^2}\right). \end{aligned} \tag{3.A.17}$$

$(\hbar\omega)^2$

The diagonal matrix element,

$$v^{ind}_{\nu\nu} \equiv -\frac{2\Lambda_\alpha^2 |\langle \nu|F|\nu\rangle|^2}{\hbar\omega_\alpha},$$

testifies to the fact, for values of $\omega_\alpha \gtrsim \omega$, with

$$\omega = |\epsilon_\nu - \epsilon_{\nu'}|/\hbar, \tag{3.A.18}$$

namely the frequencies of the single–particle excitation energy, the induced pairing interaction is attractive. Summing to (3.A.17) the matrix element of the bare interaction (3.A.3), (Fig. 3.A.3 (b))[71]

$$v^{bare}_{\nu\nu'} = \kappa \left|\langle \nu'|F|\nu\rangle\right|^2, \tag{3.A.19}$$

one obtains for the total pairing matrix element[72]

$$v_{\nu\nu'} = \boxed{v^{bare}_{\nu\nu'}(1+\chi(\omega))} = v^{bare}_{\nu\nu'}\left(1 + v^{bare}_{\nu\nu'}\Pi_{\nu\nu'}(\omega,\omega_\alpha)\right), \tag{3.A.20}$$

$$= v^{bare}_{\nu\nu'} + (v^{bare}_{\nu\nu'})^2\,\Pi_{\nu\nu'}(\omega,\omega_\alpha).$$

where

$$\Pi_{\nu,\nu'} = \begin{cases} \left(C_\alpha |\langle \nu'|F|\nu\rangle|^2\right)^{-1} \frac{\omega_\alpha^2}{\omega^2-\omega_\alpha^2}, \\ \left(D_\alpha |\langle \nu'|F|\nu\rangle|^2\right)^{-1} \frac{1}{\omega^2-\omega_\alpha^2}. \end{cases} \tag{3.A.21}$$

both expressions being equivalent in keeping with the fact that $\omega_\alpha = (C_\alpha/D_\alpha)^{1/2}$.

[71] Within the framework of (3.A.3) and of its role in (3.A.20) one finds, in the case of superconductivity in metals to be discussed below, that the bare unscreened Coulomb interaction can be written as

$$U_c(r) = \frac{1}{2}\sum_{i,j}\frac{q_i q_j}{|\mathbf{r}_i - \mathbf{r}_j|},$$

i, j running over all particles (nuclei and electrons) and $q_i = -e$ for electrons and Ze for nuclei.

[72] It is of notice that $\Pi_{\nu\nu'}$ is closely related with Lindhard's function (Lindhard (1953)). See Eq. (3.A.67) below.

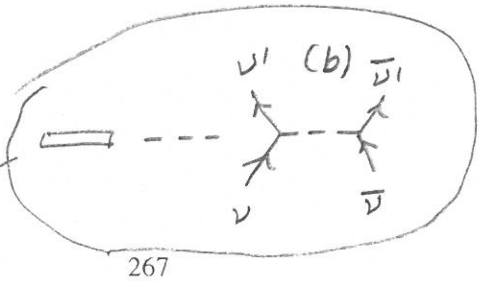

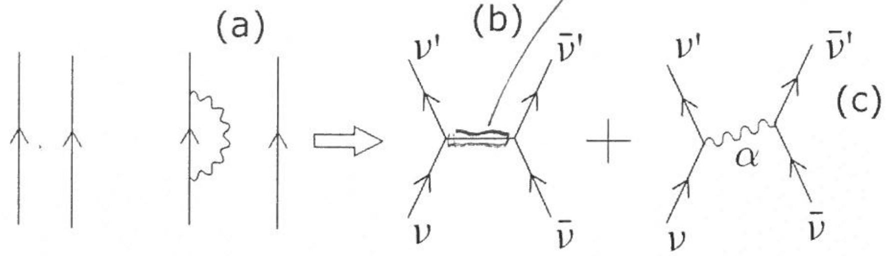

Figure 3.A.3: Starting with two bare nucleons moving around a closed shell system N_0 in Hartree–Fock orbitals (arrowed lines far left), a graphical (NFT) representation of (a) self energy processes and of (b) bare and (c) induced pairing interactions are displayed.

(ω) - (ω) handwritten nn. (267)a + (267)b

In the second expression of $\Pi_{\nu\nu'}$ the inertia of the phonon appears in the denominator, similar to the factor (Z/AM) in (3.A.67) below. It is of notice that C_α and $\hbar^2/D_\alpha$ are in MeV.

~~Let us now discuss two ($i = 1, 2$) particular situations of interest:~~

$$\text{1)} \qquad \omega = \omega_\alpha - \delta\omega/2, \quad (\delta\omega \ll \omega_\alpha), \tag{3.A.22}$$

$$\text{2)} \qquad \omega_\alpha \gg \omega. \tag{3.A.23}$$

~~That is~~

$$\lim_{\omega \to i} \frac{\omega_\alpha^2}{\omega^2 - \omega_\alpha^2} = \begin{cases} -\frac{\omega_\alpha}{\delta\omega} \ll -1 & (i = 1) \text{ plastic–}\alpha \text{ modes,} \\ 1 & (i = 2) \text{ elastic–}\alpha \text{ modes.} \end{cases} \tag{3.A.24}$$

~~The first situation is typical of low-lying collective surface vibrations and can lead $\Pi_{\nu\nu'}$. The second of high lying giant resonances. While in this last case one can parametrize the effect in terms of constant effective moments[73], the explicit treatment of the state- (ω-dependence) of the first one is unavoidable.~~

Let us ~~conclude this section by making~~ a simple estimate of the contribution of the induced pairing interaction to the (empirical) nuclear pairing gap. For this purpose ~~we introduce~~ the quantity

now carry

$$\lambda = N(0)v_{\nu\nu'}^{ind} \tag{3.A.25}$$

where $N(0)$ is the density of levels of a single spin orientation at the Fermi energy. The above quantity is known as the nuclear mass enhancement factor. This is because of the role it plays in the nucleon ω–mass (see App. 4.A and App. 4.H)

$$m_\omega = (1 + \lambda)m. \tag{3.A.26}$$

Systematic studies of this quantity, and of the related discontinuity occurring by the single–particle occupation number at the Fermi energy, namely $Z_\omega = (m/m_\omega)$ testifies to the fact that $\lambda \approx 0.4$.

~~[73]See e.g. Bohr, A. and Mottelson (1975) pp. 421 and 432.~~

København 23/07/19 (267)$_a$

(ω) to p. 267

It is of notice that $v_{\nu\nu'}$ can display a resonant behaviour leading to attraction regardless whether $v^{bare}_{\nu\nu'}$ is attractive or repulsive ($\lim_{\omega-\omega_\alpha\to 0^-} \Pi_{\nu\nu'} \to -\infty$), a situation found in the case of dielectric polarization effects in metals. In this case, the resulting effective electron - electron interaction (phonon-exchange) is attractive (see Eq. (3.A.67)), and is at the basis of Cooper pair correlation and BCS superconductivity.

Let us discuss the case of ^{11}Li, in which case Cooper pair binding results mainly from the exchange of the low-lying dipole mode between the two halo nuclei. Making use of the bare screened interaction*) $G_{scr} \approx 0.05\,G \approx 0.1$ MeV ($G \approx 28/A$ MeV) ($v^{bare}_{\nu\nu'} = -G_{scr} = -0.1$ MeV), and of the induced pairing interaction $v^{ind}_{\nu\nu'}$ ($= M_{ind} \approx -0.6$ MeV), one can write for the last term in (3.A.20), $(0.1\,\text{MeV})^2\,\Pi_{\nu\nu'}(\omega_\alpha,\omega) = -0.6$ MeV leading to $\Pi_{\nu\nu} = -60$ MeV^{-1}. This large effect is not a resonant phenomenon, although the energies $\hbar\omega$ ($= \tilde{\varepsilon}_{p1/2} - \tilde{\varepsilon}_{s1/2} \approx 0.5$ MeV) and $\hbar\omega_\alpha$ ($\gtrsim 0.7$ MeV) are rather similar, at the basis of which one finds the screening potential ($V_1 = 125$ MeV) which arising from the poor overlap between core (^{9}Li) and halo neutron wavefunctions, as in the case of G_{scr} can be assumed, for order of magnitude estimates to be equal to it (i.e. ≈ 0.05). Thus

*) see Proceedings Varenna (2019)

København 23/07/19

267b

$(V_1)_{scr} \approx 6$ MeV. Making use of the parametrization*) $\hbar\omega_\alpha = \hbar\omega_0 (1 + K/C^{(0)})^{1/2}$, where $K \approx V_1 A^{-5/3}$ MeV fm^{-2}, $C^{(0)} = 41 A^{-5/3}$ MeV fm^{-2} and $\hbar\omega_0 = 41$ MeV$/A^{1/3}$ in the case of nuclei along the stability valley, one obtains $\hbar\omega_\alpha = 41$ MeV $(1 + V_1/41)^{1/2} \approx 80$ MeV $A^{-1/3}$. In the case of ^{11}Li $\hbar\omega_0 \approx \tilde{\varepsilon}_{p1/2} - \tilde{\varepsilon}_{s1/2} \approx 0.5$ MeV, and V_1 is to be replaced by $(V_1)_{scr}$. Thus $\hbar\omega_\alpha \approx 0.5 \times (1,2)^{1/2}$ MeV ≈ 0.6 MeV.

(ω)

to p. 267

*) Bohr and Mottelson (1975) Eq. (6-315a)

F. London, The general theory of molecular forces, Transactions of the Faraday Society 33, 8 (1937).

retarded, fully quantal contribution, arising from (dipole) zero point fluctuations (ZPF) of the two interacting atoms or molecules, and the only active in the case of non–polar molecules[76], play the most important role, static-induced interactions being less important (App. 2.D). A consequence of this result is the fact that the limiting size of globular proteins ($\approx$ 50 Å) is controlled by the strong damping undergone by the retarded contribution to the amino acid interaction, when the frequency associated with the back and forth propagation of the force matches the molecules electronic frequencies[77].

Concerning superconductivity, the overscreening effect which binds weakly Cooper pairs stems from a delicate ω–dependent interaction, interaction which in the case of low temperature superconductors leads, eventually, to one of the first macroscopic manifestations of quantum mechanics, as e.g. "permanent" magnetic fields associated with persistent supercurrents.

The statement "*Life at the edge of chaos*"coined in connection with the study of emergent properties in biological molecules (e.g. protein evolution, folding and stability) reflects the idea, as expressed by de Gennes[78], that truly important new properties and results can emerge in systems lying at the border between rigid order and randomness, as testified by the marginal stability and conspicuous fluctuations characterizing, for example, nuclear Cooper pairs at the dripline and in metals, and that of proteins of e.g. viral particles like the HIV–1– and HCV–proteases[79].

Let us conclude by quoting again de Gennes but doing so with the hindsight of twenty years of nuclear research which have elapsed since "Les objets fragiles" was first published. The chapter entitled "Savoir s'arreter, savoir changer" starting at p. 180 opens with the statement *) "En ce moment, la physique nucléaire (la science des noyaux atomiques) est une science qui, à mon avis, se trouve en fin de parcours... C'est une physique qui demande des moyens coûteux, et qui s'est constituée par ailleurs en un puissant lobby. Mais elle me semble naturellement exténuée... je suis tenté de dire: "Arretons"... mais ce serait aussi absurde que de vouloir arreter un train a grande vitesse. Le mieux serait d'aiguiller ce train sur une autre voie, plus nouvelle et plus utile à la collectivité."

*) traducción Gregory

In a way, and even without knowing de Gennes remark, part of the nuclear physics community have followed them, capitalizing on the novel embodiment

[76]Within this context van der Waals and gravitation are two forces which are universally operative, acting among all bodies. In connection with quantal fluctuations and van der Waals forces, see London (1937).

[77]It is of notice that similar arguments (cf. Sect. 2.6) are at the basis of the estimate (2.6.13) concerning the size of the halo nucleus ^{11}Li, a quantity which is influenced to a large extent by the maximum distance (correlation length) over which partners of a Cooper pair are virtually (of course only if particle, normal, density allows for it) but solidly anchored to each other (localized), and have to be seen as an (extended) bosonic entity and not as two fermions. The fact that Cooper pair transfer proceeds mainly in terms of successive transfer controlled by the single–particle mean field, reinforces the above physical picture of nuclear pairing. Even under the effect of extremely large, as compared to the pair correlation energy, external single–particle fields, namely that of target and projectile, the Cooper pair field extends over the two nuclei, permeating the whole summed nuclear volume also through tiny density overlaps.

[78]de Gennes (1994).

[79]See e.g. Broglia, R. A. (2013).

quantum

that concepts like elementary modes of excitation, spontaneous symmetry breaking and phase transitions have had in this paradigm of finite many-body (FMB) system the nucleus represents, where fluctuations can dominate over potential energy effects. The use of these concepts tainted by FMB system effects as applied to proteins, in particular to the understanding of protein folding may, arguably, shed light on the possibility of designing leads to drugs which are less prone to create resistance[80], let alone all the parallels that one has been able to establish and the associated progress resulting from them concerning cluster and quantum dots physics, a particular example being the discovery of super shells[81]. Q Q

3.A.2 Metals

Plasmons and phonons (jellium model)

The expression of the electron plasmon (ep) frequency of the antenna–like oscillations of the free, conduction electrons of mass m_e and charge $-e$, against the positive charged background (jellium model) is

3

$$\omega_{ep}^2 = \frac{4\pi n_e e^2}{m_e} = \frac{3e^2}{m_e r_s^2}, \tag{3.A.31}$$

where

$$n_e = \frac{3}{4\pi}\frac{1}{r_s^3}, \tag{3.A.32}$$

are the number of electrons per unit volume, r_s being the radius of a sphere whose volume is equal to the volume per conduction electron,

$$r_s = \left(\frac{3}{4\pi n_e}\right)^{1/3}, \tag{3.A.33}$$

that is, the radius of the Wigner–Seitz cell.

For[82] metallic Li

$$n_e = 4.70\frac{10^{22}}{\text{cm}^3} = \frac{4.7\times 10^{-2}}{\text{Å}^3}, \tag{3.A.34}$$

while

$$r_s = \left(\frac{3\text{Å}^3}{4\pi\times 4.7\times 10^{-2}}\right)^{1/3} = 1.72\text{Å}, \tag{3.A.35}$$

implying a value $(r_s/a_0) = 3.25$ in units of Bohr radius ($a_0 = 0.529$Å). Making use of

$$\alpha = 7.2973\times 10^{-3} = \frac{e^2}{\hbar c} \tag{3.A.36}$$

[80] See e.g. Broglia, R. A. (2013); Broglia (2005); Rösner et al. (2017) and refs. therein.

[81] Pedersen et al. (1991); de Heer et al. (1987); Brack (1993); Pacheco et al. (1991); Lipparini (2003); Martin et al. (1994); Bjornhølm et al. (1994).

[82] cf. page 5, table 1.1 of Ashcroft and Mermin (1987).

and

$$e^2 = 14.4\,\text{eV Å}, \tag{3.A.37}$$

one obtains

$$\hbar c = \frac{14.4\,\text{eV Å}}{7.2973 \times 10^{-3}} = 1973.3\,\text{eV Å}. \tag{3.A.38}$$

Making use of the above values and of

$$m_e c^2 = 0.511\,\text{MeV}, \tag{3.A.39}$$

one can write

$$\hbar^2 \omega_{ep}^2 = \frac{(\hbar c)^2}{m_e c^2}\frac{3e^2}{r_s^3} = \frac{(1973.3\,\text{eV Å})}{0.511 \times 10^6\,\text{eV}}\frac{3 \times 14.4\,\text{eV Å}}{(1.72\,\text{Å})^3} = 64.7\,\text{eV}^2 \tag{3.A.40}$$

leading to[83]

$$\hbar\omega_{ep} = 8.04\,\text{eV} \approx 1.94 \times 10^9\,\text{MHz} \tag{3.A.41}$$

For the case of metal clusters of Li, the Mie resonance frequency is *)

$$\hbar\omega_M = \frac{\hbar\omega_{ep}}{\sqrt{3}} = 4.6\,\text{eV}. \tag{3.A.42}$$

3.A.3 Elementary theory of phonon dispersion relation

Again, within the framework of the jellium model, one can estimate the long wavelength ionic plasma (ip) frequency introducing, in (3.A.31) the substitution $e \to Ze$, $m_e \to AM$ ($A = N + Z$, mass number, M nucleon mass), $n_e \to n_i = n_e/Z$,

$$\omega_{ip}^2 = \frac{4\pi n_i (Ze)^2}{AM} = \frac{Zm_e}{AM}\omega_{ep}^2, \tag{3.A.43}$$

$AM(Ze)$ being the mass (charge) of the ions[84]. For metallic Li, one obtains

$$\hbar\omega_{ip} = \left(\frac{Zm_e}{AM}\right)^{1/2} \hbar\omega_{ep} = \left(\frac{3 \times 0.5}{9 \times 10^3}\right)^{1/2} \times 1.94 \times 10^{15}\,\text{sec}^{-1}$$
$$\approx 2.5 \times 10^{13}\,\text{sec}^{-1} \approx 10^{13}\,\text{sec}^{-1} \approx 1.04 \times 10^2\,\text{meV}. \tag{3.A.44}$$

Now, both the relations (3.A.31) and (3.A.43), although being quite useful, are wrong from a many–body point of view: ω_{ep} because electrons appear as bare electrons not dressed by the phonons, neither by the plasmons; ω_{ip} because the static negative background does not allow for an exchange of electron plasmons between ions, exchange eventually leading to a screened, short–range ionic Coulomb repulsive field. Namely ions interact, in the approximation used above, in terms of the "bare" ion–ion Coulomb interaction. Being it infinite range it does not allow for a

[83] Kittel (1996) Table 2, p. 278.

[84] Ketterson and Song (1999), p. 230.

*) See Bertsch and Broglia ( ), Sect. 5.1, also Table 5.1.